

The Brain’s Bitter Lesson: Scaling Speech Decoding With Self-Supervised Learning

Dulhan Jayalath¹ Gilad Landau¹ Brendan Shillingford²

Mark Woolrich³ Oiwi Parker Jones¹

{¹PNPL, ³OHBA}, University of Oxford ²Google DeepMind
 {dulhan, oiwi}@robots.ox.ac.uk

Abstract

The past few years have produced a series of spectacular advances in the decoding of speech from brain activity. The engine of these advances has been the acquisition of labelled data, with increasingly large datasets acquired from single subjects. However, participants exhibit anatomical and other individual differences, and datasets use varied scanners and task designs. As a result, prior work has struggled to leverage data from multiple subjects, multiple datasets, multiple tasks, and unlabelled datasets. In turn, the field has not benefited from the rapidly growing number of open neural data repositories to exploit large-scale data and deep learning. To address this, we develop an initial set of neuroscience-inspired self-supervised objectives, together with a neural architecture, for representation learning from heterogeneous and unlabelled neural recordings. Experimental results show that representations learned with these objectives scale with data, generalise across subjects, datasets, and tasks, and are also learned faster than using only labelled data. In addition, we set new benchmarks for two foundational speech decoding tasks. Taken together, these methods now unlock the potential for training speech decoding models with orders of magnitude more existing data.

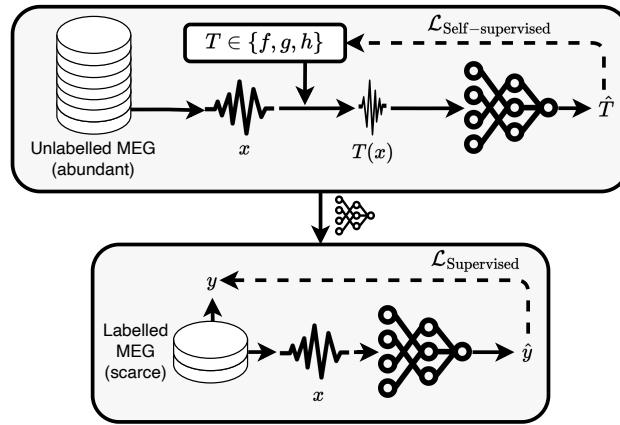


Figure 1: **Leveraging unlabelled data for speech decoding.** We pre-train a neural network using tasks that generate implicit labels from abundant unlabelled neuroimaging data, permitting learning from large heterogeneous datasets. The tasks apply a randomly selected transformation T to the data and the network predicts the transformation. We fine-tune the pre-trained network on labelled data, achieving faster generalisation owing to the strength of the representation learned in pre-training.

1 Introduction

In his *Bitter Lesson*, Richard Sutton argues that a major conclusion of 70 years of AI research is that general methods exploiting large-scale computation will outperform model-based approaches as the availability of compute increases [50]. In line with this, the generality of deep learning, via statistical learning from ever bigger datasets, has allowed the field to leverage computation in a way that appears to scale arbitrarily, leading to astounding advances across a diverse set of domains [29, 7, 42, 46].

In the domain of brain data, and of tasks like speech decoding, the bitter lesson has not yet been fully assimilated. State-of-the-art *brain-computer interfaces (BCIs)* have tried to scale up labelled datasets for individual subjects, using either invasive [40, 60] or non-invasive brain recordings [52], mapping these to transcripts of attempted or imagined speech. Yet, a number of obstacles to scale remain. With few exceptions at present (e.g. [17]), speech decoding models tend not to train on data from more than one subject. Moreover, they do not combine data from multiple datasets and in general do not utilise unlabelled data, or data from diverse tasks. Thus the size of training data has been limited to how much can be acquired for a single subject, and data from other subjects, or from the growing number of public data repositories, has not been leveraged. There are many reasons for these limitations; individual brains and data from different neuroimaging scanners differ, for example. But overcoming these limitations, as has begun to happen in neighbouring sub-fields (e.g. [27]), holds the promise of training models on collective, internet-scale data.

Given the scarcity of labelled data, *self-supervised learning (SSL)* appears promising as an avenue for domains where such data is rare or hard to obtain [3]. In the SSL paradigm, *pretext* tasks pre-train a model on unlabelled data by generating implicit training labels through transformations of the input data in order to help a downstream task. We develop a set of these tasks, informed by advances in neuroscience, for learning with unlabelled brain data (Figure 1) and design an architecture for processing continuous multi-sensor neuroimaging signals. In order to scale existing non-invasive datasets, we provide a unified method that allows us to leverage data from other experiments that do not have the same labels (by treating them as unlabelled) and that come from different subjects and neuroimaging scanners. We evaluate the representations learned with our approach on heard speech datasets acquired with non-invasive *magnetoencephalography (MEG)*, setting the baselines for speech detection and voicing classification on this data. The results not only demonstrate that scaling with unlabelled data works in speech decoding, but also shows that these representations can generalise across datasets, tasks, and even novel subjects for the first time. Our main contributions are:

- A set of domain specific **self-supervised pretext tasks** for representation learning that can scale speech decoding over multiple subjects, multiple studies, and unlabelled data;
- A **neural architecture** for learning these self-supervised objectives and training downstream speech decoding from brain data; and
- A comprehensive **experimental evaluation** providing evidence that our approach can scale up with data and enable cross-dataset, task, and subject generalisation.

2 Related Work

Prior work in speech decoding has focused almost entirely on supervised learning with decoding models that typically do not generalise across participants or experiments. This is true both in recent state-of-the-art invasive studies [40, 39, 60, 9] and non-invasive studies [52]. These prior works have scaled up the experimental data collected within individual subjects, but are unable to leverage data from other subjects and experiments. Focusing on semantic rather than phonetic decoding, work by Tang et al. [52] is remarkable for showing an ability to generalise across labelled task data when listening to speech, imagining speech, or even watching videos. They do not, however, leverage unlabelled data and are unable to show generalisation between subjects.

Specific studies into the limitations of generalising models between subjects show that while performance decreases on average when subjects are pooled, there are exceptions. Csaky et al. [11] find that a subset of individuals perform better when evaluated with a group-level model than with individual models. Exploiting audio data in a multi-modal framework, Défossez et al. [17] show that decoding performance improves for a segment identification task as data from multiple subjects listening to connected speech are aggregated. Although they repeat the result within two MEG

and two EEG datasets, Défossez et al. [17] do not show any improvements for pooling data across datasets. Moreover, they do not combine data from studies with different labels either; cf. [58, 16, 56]. Unfortunately, two of these papers [58, 16] included a bug in their evaluation code. As such, their methods may perform no better than a baseline that provides pure noise inputs to the model [28].

In general, speech decoding has centred on different kinds of speech: listening, imagining, speaking out loud, and, for paralysed patients, attempting to speak aloud. We focus here on listening because it is easier to decode than imagined speech (e.g. [37]). There is also some evidence of a functional overlap between listening and imagined speech representations in the brain [55], though we acknowledge that the question of overlap has been contested [30]. Prior work has also investigated the two tasks that we focus on here [13, 40, 23]. The first of these, speech detection, formed the backbone to Moses et al. [40], where a speech detection model was trained and subsequently used to detect isolated words, which were in turn classified and checked against a language model to generate acceptable sentences. Hamilton et al. [26] further elaborated on the neural anatomy underlying speech detection, categorising neural responses in the *superior temporal gyrus (STG)* to sustained speech and speech onset. As for the second task, voicing classification, Gwilliams et al. [23] used this task as a proxy for phoneme classification, as pooling phonemes into unvoiced or voiced segments (e.g. /p t k f s/ vs /b d g v z/) improves data efficiency. We note that voicing classification and speech detection are related tasks as voicing is a subclass of speech. This makes them foundational for building hierarchical speech decoding pipelines similar to prior surgical decoding work [40, 60].

In the computer vision literature, there have been a plethora of methods that use self-supervised pretext tasks for representation learning [1, 15, 41, 31, 62, 21]. Until now, similar approaches have not translated to the brain decoding literature. However, prior work has used other methods to leverage unlabelled brain data. For example, Jiang et al. [27] succeeded in cross-dataset and cross-task generalisation, using a transformer with tokenised brain signals and a masked token prediction objective. Although this work combined unlabelled EEG datasets, it only achieved improvements on non-speech tasks. Wang et al. [57] used a similar approach, replacing tokens with contextualised embeddings of time-frequency input representations. They attained impressive speech detection results but with invasive neural recordings, which are comparatively rare and thus have much less potential to scale than non-invasive data.

3 Method

To process continuous neuroimaging data, we introduce a neural architecture for encoding heterogeneous brain signals into latent representations. By developing pretext tasks with the objective of learning generalisable brain representations, we leverage this architecture for self-supervised learning from unlabelled data, hoping to replicate similar successes in computer vision [21, 8].

3.1 Network Architecture

We design a two-stage neural network architecture (Figure 2). The pre-training stage uses pretext tasks to train a representation with unlabelled brain data. Then, the fine-tuning stage uses this representation to learn the downstream task by fine-tuning with labelled data.

Normalisation. We divide recordings into windows of length w seconds or t samples. At train time, each batch of windows is standardised such that each sensor has zero mean and unit variance.

Backbone. The network takes as input the standardised sample windows. To combine heterogeneous datasets, which have different numbers of sensors S , we apply a dataset-conditional linear layer to the sensor dimension, projecting the signal into a shared space with dimension d_{shared} . Then, to encode the signal, we construct a wave-to-wave convolutional encoder architecture, the *cortex encoder*, inspired by work in neural audio codecs [61, 14]. Specifically, our convolutional encoder adapts the implementation of the SEANet architecture [51] used in Défossez et al. [14]. As these codecs typically operate on mono audio signals in $\mathbb{R}^{1 \times t}$, while our signals are in $\mathbb{R}^{d_{\text{shared}} \times t}$, we increase the convolutional channel dimension from 1 to match d_{shared} while also inflating the channel dimension of subsequent convolutions. We refer to the output dimension of embeddings from this backbone as d_{backbone} . Thus, the backbone takes as input a window in $\mathbb{R}^{S \times t}$, and encodes this into τ embeddings (where $\tau < t$), each of dimension d_{backbone} (i.e. an $\mathbb{R}^{d_{\text{backbone}} \times \tau}$ output).

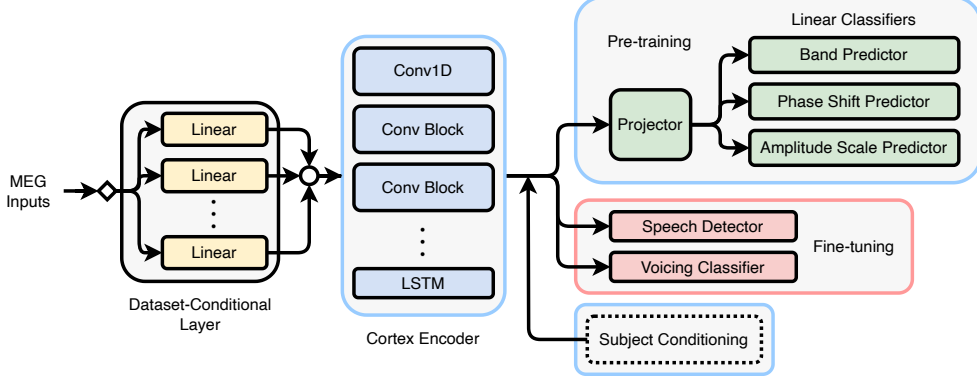


Figure 2: **Architecture overview.** Inputs are projected into a shared dimension, then encoded. In pre-training, all weights are trainable except for modules in light-red, while in shallow fine-tuning, modules with light-blue borders are frozen and modules with light-red borders are unfrozen. Deep fine-tuning is identical, except the encoder is trainable. Dashed borders indicate optional components.

Pre-training. Following the advice of Balestrieri et al. [3, Section 3.2], we use a two-layer feedforward projector to alleviate misalignment between our pretext and downstream tasks in the representation. After the projector, linear classifiers make predictions for each of the pretext tasks.

Fine-tuning. In this stage, we introduce classifiers for the downstream tasks and train with labelled data and supervised learning (Figure 2). Depending on the experiment, we fine-tune in one of two ways. In the first, we train an MLP classifier from scratch on top of the pre-trained representation, which remains frozen. Thus, we backpropagate only through the classifier. We call this *shallow fine-tuning*. In the other, we fine-tune by training an MLP on top of the pre-trained representation again, but do not freeze the backbone, training end-to-end. Here, we backpropagate through the classifier *and* the backbone. We refer to this as *deep fine-tuning*. In both cases, a new trainable dataset-specific linear layer can be introduced for a novel dataset.

For speech detection, our classifier makes a prediction for each individual embedding. For voicing classification, where there is only one label for each sample window, the embeddings are flattened into a tensor in $\mathbb{R}^{d_{\text{backbone}} \times \tau}$ representing the entire window. This is the input to the voicing classifier and is referred to as full epoch decoding in neuroimaging literature [12].

Subject conditioning. Just as speakers have different voices, neural responses between subjects have different characteristics. Consequently, individual variation leads to models that do not generalise well across subjects [11]. In the speech literature, models include speaker conditioning to account for these differences [20]. We take a similar approach by introducing subject conditioning, represented as a subject embedding, to our model. With a SEANet-based architecture, Zeghidour et al. [61] find that conditioning is equally as effective at the encoder bottleneck as in other stages of the model. Hence, we place ours at the cortex encoder bottleneck for simplicity. We evaluate multiple types of conditioning including subject embeddings and *feature-wise linear modulation (FiLM)* [44].

3.2 Pretext Tasks

Our pretext tasks are unsupervised feature learning tasks for continuous neuroimaging signals that aim to learn generalisable speech decoding features. Since different datasets use different hardware and varied numbers of sensors, we construct these tasks with labels that are agnostic to the number of sensors in the signal. This means that these tasks do not require identifying specific sensor channels.

Band prediction. In the literature, neural responses can be broadly segmented into functional frequency bands [22, 45, 36]. *Delta* (δ) waves (0.1–4 Hz) are commonly associated with the rhythmic structure of heard speech [35], *Theta* (θ) waves (4–8 Hz) reliably track [34] and phase-lock to the amplitude envelope of heard sentences [43], *Alpha* (α) waves (8–12 Hz) relate to attentional processes and the inhibition of irrelevant information, helping to focus on relevant speech signals [49], *Beta* (β) waves (12–30 Hz) are implicated in top-down predictive coding [5] which affects lexical processing [59], *Gamma* (γ) waves (30–70 Hz) occur with higher cognitive functions (e.g. memory,

learning, reasoning, and planning) [19, 6], and *High Gamma* (γ^{high}) waves (>70 Hz) have been linked specifically to speech detection [26] and phonemic feature classification in the STG [38] as well as phonemic feature classification in the *ventral sensorimotor cortex* (*vSMC*) [10]. As High Gamma is a relatively wide band, we have split it into two sub-bands: *Lower High Gamma* ($\gamma_{\text{lower}}^{\text{high}}$) waves (70–100 Hz) and *Upper High Gamma* ($\gamma_{\text{upper}}^{\text{high}}$) waves (100–150 Hz).

To learn representations that can distinguish between these, our band prediction task applies a band-stop filter for a randomly selected band ω to the sample x , passes the filtered sample $x^{\omega'}$ through the network backbone g and the corresponding predictor f_{band} , requiring the network to predict the frequency band that was rejected. This yields the loss

$$\mathcal{L}_{\text{band}} = \sum_{x \in B} \mathcal{L}_{\text{CE}}(f_{\text{band}}(g(x^{\omega'})), \omega), \quad (1)$$

where B is a mini-batch of samples, $\omega \in \{\delta, \theta, \alpha, \beta, \gamma, \gamma_{\text{lower}}^{\text{high}}, \gamma_{\text{upper}}^{\text{high}}\}$, and \mathcal{L}_{CE} is the cross-entropy loss as this is a multi-class classification task.

Phase shift prediction. Phase coupling between networks of neuron populations is necessary for coordinating brain activity [18, 54]. Thus, since phase often synchronises between communicating brain areas, phase coupling between spatially distant sensors is likely to be a useful feature. Supporting this insight, recent work [27] also finds phase to be an essential component of the signal.

To learn representations that encode phase differences between brain areas, this task applies a discrete uniform random phase shift $\phi \in \{0, \frac{\pi}{8}, \frac{\pi}{4}, \frac{3\pi}{8}, \frac{\pi}{2}, \frac{5\pi}{8}, \frac{3\pi}{4}, \frac{7\pi}{8}\}$ to a uniformly randomly selected proportion ρ of the sensors. Applying this shift to random sensors is critical since sensors are placed in different positions, capturing different regions of the brain. Uniform random selection ensures differences between any two regions of the brain are represented. The objective of this task is to predict the phase shift. This leads to a similar loss

$$\mathcal{L}_{\text{phase}} = \sum_{x \in B} \mathcal{L}_{\text{CE}}(f_{\text{phase}}(g(x^\phi)), \phi), \quad (2)$$

where x^ϕ describes the signal with a phase shift ϕ applied to a proportion of the sensors. We use a discrete number of possible phase shifts, treating it as a multi-class task rather than a regression task, to ease the difficulty of the problem as MEG scanners typically have a large number of sensors.

Amplitude scale prediction. MEG and EEG signals use an array of sensors at different spatial locations, capturing different signal sources more intensely. Representing the relative amplitude difference between sensors could be important for differentiating between neural responses originating from distinct parts of the brain. Within speech, Hamilton et al. [26] find that localised regions of the STG respond to sustained speech and speech onsets. Differentiating between neural responses from this region and others may be essential for decoding speech perception.

Thus, this pretext task focuses on learning representations that encode relative sensor amplitude differences. Similar to the phase shift task, we select a random proportion of the sensors ρ and apply a discrete random amplitude scaling coefficient $A \in [-2, 2]$, discretised into 16 scaling factors, to the signal. The objective is to predict the scaling factor, leading to the loss

$$\mathcal{L}_{\text{amplitude}} = \sum_{x \in B} \mathcal{L}_{\text{CE}}(f_{\text{amplitude}}(g(x^A)), A), \quad (3)$$

where x^A is the signal scaled with A .

These pretext tasks capture complementary time- and frequency-domain properties of the signal. Hence, during pre-training, we combine them, creating an augmented version of the input for *every* pretext task by applying the matching transformation. We feed the augmented inputs through the network backbone and apply the corresponding classifier to predict the transformation, summing the weighted losses such that our final pre-training loss is given by

$$\mathcal{L}_{\text{SSL}} = w_1 \mathcal{L}_{\text{band}} + w_2 \mathcal{L}_{\text{phase}} + w_3 \mathcal{L}_{\text{amplitude}}, \quad (4)$$

where w_i is a constant coefficient for each self-supervised loss.

4 Experiments

In this section, we evaluate the representations learned with our pretext tasks by measuring their ability to scale downstream performance with unlabelled data. This includes understanding how well they can generalise across datasets, subjects, and tasks. We focus our evaluation on MEG data as the signal is rich, with better spatial resolution than EEG [32] and faster sampling rates than fMRI [25].

4.1 Experimental setup

Datasets. Unless specified otherwise, our experiments use Cam-CAN [48, 53] as an unlabelled representation learning dataset for pre-training. This is a study containing 641 subjects with resting and sensorimotor tasks, totalling approximately 160 hours of MEG recordings. For our downstream tasks, we use two labelled heard speech MEG datasets where participants listen to short stories or audiobooks. Armeni et al. [2] contains 3 subjects who listen to 10 hours of recordings each (30 hours total) while Gwilliams et al. [24] has 27 subjects, each recorded for 2 hours (54 hours total). Overall, we utilise over 200 hours of data. To the best of our knowledge, this is the largest volume of MEG data ever used for speech decoding.

Preprocessing. Each recording is in $\mathbb{R}^{S \times T}$ where S is the number of sensors and T is the number of time points sampled by the scanner. To eliminate high-frequency muscle movement artifacts, we apply a low-pass filter at 125Hz as well as a high-pass filter at 0.5Hz to remove slow-drift artifacts. Since the datasets were recorded in Europe, where the electric grid frequency is 50Hz, we apply a notch filter at multiples of 50Hz to account for line noise. Next, we downsample the signal to 250Hz, avoiding aliasing at frequencies up to our low-pass filter threshold. Finally, we detect bad sensor channels, those with significant noise and artifacts, using a variance threshold and replace them by interpolating the spatially nearest sensors.

Downstream tasks. We evaluate our methods with two fundamental speech decoding tasks of increasing difficulty. The first, *speech detection*, determines whether speech occurs in the auditory stimulus using the neural response. The second task is *voicing classification*. Given data aligned at the occurrence of a phoneme, the task is to recognise whether the phoneme is *voiced* or *voiceless*, where voicing is a binary phonetic feature that categorises whether a speech sound is associated with vocal cord vibration. We select these tasks as they are simpler than phoneme recognition, but are foundational because they must be solved to decode speech accurately into natural language.

Training. We pre-train all models to completion and then shallow or deep fine-tune on labelled data for each task, using this to analyse the generalisability of the pre-trained representation. Appendix E provides complete training details for all experiments.

4.2 Learning Generalisable Representations Using Pretext Tasks

We investigate whether our self-supervised objectives produce useful representations by first learning a representation with each pretext task independently and then analysing its downstream generalisation using shallow fine-tuning (i.e. with the representation frozen). In Table 1, we show that all of our pretext tasks lead to better than chance accuracy on speech detection, and critically, outperform a randomly initialised and shallow fine-tuned baseline. The results are statistically significant in all cases, providing initial evidence that all of our tasks are helpful in learning representations that generalise downstream to speech decoding.

Interestingly, the combination of all pretext tasks leads to better generalisation than any task on its own. As we hypothesised earlier, this may be because our pretext tasks capture complementary properties in time- and frequency-space, enforcing that our representation includes more salient features for speech decoding. For our other downstream task, voicing classification, we were not able to use shallow fine-tuning to generalise to a statistically significant degree with any of the pretext tasks nor with a random backbone. It may be too difficult to learn with shallow fine-tuning and so we turn to using deep fine-tuning for this task in the next section.

Among the pretext tasks, band prediction performs best. This could be because the representation easily identifies phase-locking to speech onset in theta waves [43]. However, further investigation is necessary to determine which frequency band is most informative. The choice of the proportion of sensors to apply transformations to, $\rho = 0.5$ for phase shift prediction and $\rho = 0.2$ for amplitude

Table 1: **Pre-training with pretext tasks produces generalisable representations.** We provide the test accuracy at the point of best validation accuracy (early stopping). In the *none* baseline, the network backbone is randomly initialised before fine-tuning (i.e. there is no pre-training). When *all* pretext tasks are used, their losses are weighted equally. The uncertainty is the standard error of the mean over three random seeds. We quote the *t*-score and *p*-value for each result from a one-sample one-sided *t*-test where the population mean is chance-level accuracy. Models are pre-trained on all of Cam-CAN [48, 53] and fine-tuned on Armeni et al. [2] or Gwilliams et al. [24] respectively.

Pretext task	Speech detection balanced accuracy					
	Armeni	<i>t</i>	<i>p</i>	Gwilliams	<i>t</i>	<i>p</i>
Amp $(\rho = 0.2)$	0.5846 \pm 0.0032	26	7e-4	0.5116 \pm 0.0004	29	6e-4
Phase $(\rho = 0.5)$	0.5831 \pm 0.0029	29	6e-4	0.5093 \pm 0.0014	7	1e-2
Band	0.5941 \pm 0.0024	39	2e-3	0.5177 \pm 0.0028	6	1e-2
All	0.6011 \pm 0.0018	56	2e-4	0.5206 \pm 0.0010	22	1e-3
None (rand. backbone)	0.5000 \pm 0.0000	—	—	0.5000 \pm 0.0000	—	—
Chance-level	0.5	—	—	0.5	—	—

prediction, were determined through a hyperparameter search (Appendix F). We conjecture that a smaller ρ is optimal for amplitude scale prediction since this leads to representations that are especially strong at discriminating amplitude differences among small groups of sensors. Perhaps this makes it easier to distinguish between neural responses from distinct parts of the brain such as the STG, which is associated with speech onset [26]. In contrast, a larger ρ for phase shift prediction may be best because phase is descriptive of neural synchrony which is distributed across the brain. Unlike localised responses, a large proportion of the sensors can detect this feature.

Whilst we have shown that our representations generalise, do they outperform supervised baselines when trained to saturation? Using shallow fine-tuning once more, we compare our approach directly to similarly parameterised supervised classifiers in Table 2. A representation pre-trained with all pretext tasks significantly outperforms chance, a randomly initialised backbone, and supervised training on both downstream datasets. Here, the supervised classifier has significantly more parameters than the models that probe the network backbone because the input dimension is far larger without an encoder. Even with this bias favouring the supervised classifier, the self-supervised case performs better. Thus, it is apparent that pre-training with unlabelled data significantly improves downstream generalisation.

Table 2: **Self-supervised pre-training outperforms supervised classifiers.** We use shallow fine-tuning on top of a randomly initialised and pre-trained backbone, comparing these to a supervised classifier trained to completion. We quote test accuracy at the point of best validation accuracy (early stopping) and show uncertainty as the standard error of the mean from three seeds. We calculate the *t*-score and *p*-value from one-sample one-sided *t*-tests where the population mean is chance. Self-supervised models are pre-trained on all of Cam-CAN [48, 53] and shallow fine-tuned on Armeni et al. [2] or Gwilliams et al. [24] while the supervised models are trained entirely on the latter datasets.

Model	Speech detection balanced accuracy					
	Armeni	<i>t</i>	<i>p</i>	Gwilliams	<i>t</i>	<i>p</i>
Supervised						
Linear	0.5222 \pm 0.0015	12	3e-3	0.5006 \pm 0.0001	5	2e-2
Self-supervised + fine-tuning						
Random backbone						
MLP (two layers)	0.5000 \pm 0.0000	—	—	0.5000 \pm 0.0000	—	—
Pre-trained backbone						
Linear	0.5853 \pm 0.0017	52	3e-4	0.5011 \pm 0.0001	9	6e-3
MLP (two layers)	0.6011 \pm 0.0018	56	2e-4	0.5206 \pm 0.0010	22	1e-3
Chance-level	0.5	—	—	0.5	—	—

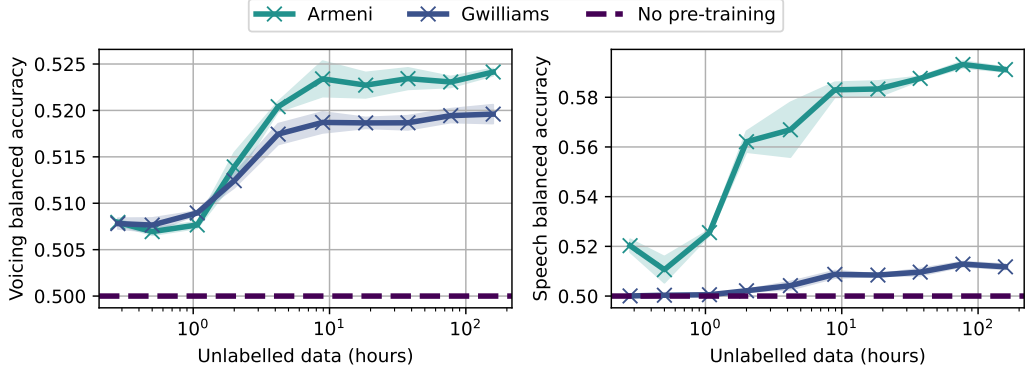


Figure 3: **Scaling unlabelled data improves downstream generalisation.** We pre-train the model on increasing amounts of unlabelled data from Cam-CAN [48, 53] and fine-tune on voicing and speech detection on the Armeni et al. [2] and Gwilliams et al. [24] datasets. *No pre-training* shows best test accuracy for a randomly initialised network fine-tuned for the same number of epochs (i.e. without pre-training). We show only one *no pre-training* line as the result is the same for both datasets. The shaded area shows the standard error of the mean across three seeds.

4.3 Scaling Speech Decoding With Unlabelled Data

Previously, we showed that the combination of all pretext tasks leads to the best representations and that this outperforms a randomly initialised backbone as well as a supervised classifier. In this section, we examine how these pretext tasks fare as we increase the amount of unlabelled data, analysing scaling performance on downstream tasks. As before, we pre-train with the combined pretext tasks using Cam-CAN [48, 53], which does not have any speech decoding labels, and now fine-tune for ten epochs on Armeni et al. [2] and Gwilliams et al. [24], showcasing transfer with minimal fine-tuning. This simulates the scenario in which models need to generalise quickly with very little calibration data from new patients in order to be deployed as a speech BCI. Where earlier we analysed only speech detection, here, we also focus on voicing classification by using deep fine-tuning for this task only. As evidenced by Section 4.2, we require this because voicing classification is a more difficult task, necessitating end-to-end training with more parameters to observe generalisation.

Figure 3 shows balanced accuracy as we increase the amount of unlabelled data in pre-training up to approximately 160 hours. For both tasks, pre-training outperforms the no pre-training baseline, which fails to generalise at all, showing that any unlabelled data is sufficient to pre-train a useful representation. In both tasks, there is a clear improvement in accuracy as the amount of unlabelled data increases. Thus, adding unlabelled data improves generalisation and scales performance. With speech detection, the improvement in accuracy is more significant for Armeni et al. [2]. Noting that there is more within-subject data in this dataset than Gwilliams et al. [24], speech detection may be more sensitive to subject variation than voicing classification.

We scaled up the pre-training dataset by increasing the number of subjects. Since this led to consistent and almost monotonic improvements in downstream accuracy, our self-supervised method is an exception to the common consensus that pooling subjects worsens generalisation. Moreover, as we pre-trained our model with a *different* dataset to those we fine-tuned on, our representation shows *cross-dataset generalisation*. This is particularly notable as the Armeni et al. [2], Gwilliams et al. [24], and pre-training datasets all use different scanners entirely. Performing well across these datasets indicates that, together, our architecture and pretext tasks successfully generate representations that are generalisable across heterogeneous scanners.

Beyond hardware, our results also show improvements on *distinct* tasks, namely speech detection and voicing classification, thus illustrating *cross-task generalisation*. Thus, our pretext tasks are sufficiently generic to produce representations that generalise to multiple downstream tasks, indicating their applicability to speech decoding more generally. Finally, our pre-training dataset contained no language data whatsoever yet still improved downstream accuracy on language tasks. Remarkably, this shows that brain data collected from *any* task (including those that are not linguistic) can be used to scale downstream speech decoding performance.

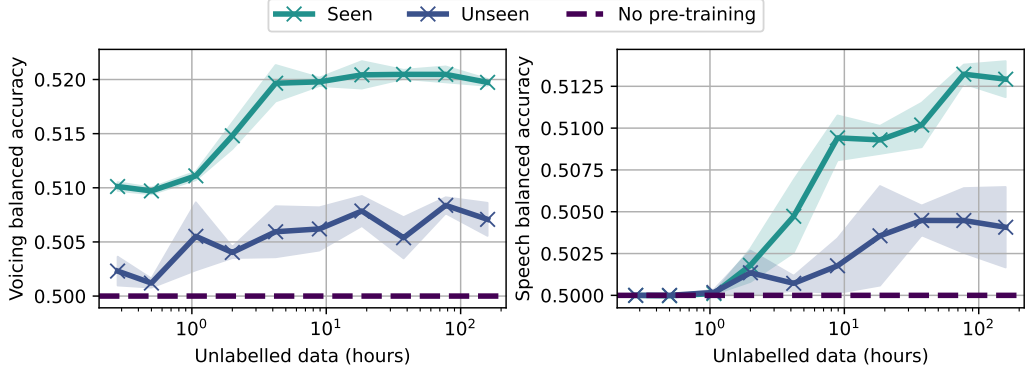


Figure 4: **Scaling pre-training data improves novel subject generalisation.** As before, we pre-train with increasing amounts of unlabelled data from Cam-CAN [48, 53], but now fine-tune only on Gwilliams et al. [24]. In the *seen* case, we evaluate on held-out sessions from subjects that were used in the training data. For the *unseen* case we evaluate on three completely held-out subjects. *No pre-training* shows the best test accuracy for a randomly initialised network fine-tuned for the same number of epochs (i.e. without pre-training). We show only one *no pre-training* line as the result is the same for both datasets. The shaded area is the standard error of the mean over three seeds.

4.4 Scaling Unlabelled Data Improves Zero-Shot Generalisation To Novel Subjects

Brain data is variable across participants, leading to difficulty transferring models to novel subjects [11]. Whilst we have shown generalisation *across* subjects with our method, here, we investigate how well we can generalise to *novel* subjects—an even more difficult challenge. This is critical in order to widely deploy speech BCIs for new patients. In the following experiment, we pre-train using the same setup as Figure 3, but fine-tune only on Gwilliams et al. [24]. We use FiLM conditioning as this performs best for seen and unseen subjects (Appendix B). During training, we hold out three subjects with which we evaluate novel subject generalisation (i.e. unseen subject performance).

Figure 4 shows that scaling up the amount of unlabelled data used in pre-training not only improves accuracy on subjects previously seen, but also demonstrates a positive trend in performance for unseen (novel) subjects. This is a promising result, indicating that scaling with our method is an encouraging direction for resolving the issues related to individual variance faced by prior work.

4.5 Limitations

Although our results are significant in demonstrating a viable path forward to scale up speech BCIs, there remain a number of limitations to the present work. We focused here on two downstream tasks: speech detection and voice classification. Ultimately, we would like to expand this work to predict full transcripts from brain recordings (i.e. *brain-to-text*). This has been achieved with surgical data [40, 60] but not yet convincingly with non-invasive methods like MEG or EEG [28]. Speech detection has played an important role in the development of full brain-to-text in a surgical context [40] and we hope may play a similar role for non-invasive methods. Prior work has further used voice classification as a stand in for phoneme classification [23], and we have been able to improve on these results here. In future work, we would like to expand this to all English phonemes. Secondly, while we have been able to demonstrate the utility of a few pretext tasks here, we do not claim to have exhausted the full set of useful tasks. Rather, we conjecture that more useful pretext tasks remain to be found and believe a useful avenue of research will be into other input representations for brain recordings. For example, this paper did not make use of spatial features. Another limitation is our emphasis on heard speech over other types of speech, such as attempted or imagined speech. We hypothesise that the same methods presented here will generalise to these other varieties of speech, though this has yet to be shown. But, perhaps the biggest limitation of the present work is that, while it surpasses the amount of data used in other studies, it remains to be seen how much speech decoding tasks can be improved by scaling up the number of datasets used in training. In sharing this work now, we believe that the current proof of concept will be sufficiently impactful to the field as we continue to actively scale up the datasets that we can leverage.

5 Conclusion

Ultimately, solving speech decoding could transform the lives of patients with severe communication difficulties. Yet, this promise has not materialised because the field has been blocked by its inability to scale up data to leverage deep learning. Prior methods have been unable to aggregate data across different datasets, labels, or subjects to scale up because of heterogeneity in recording hardware, experiment design, and participants. A handful of studies have shown weak signals towards alleviating these issues. But until now, no one has developed a general solution. We provided a unified method that leverages unlabelled data using generic pretext tasks that shows that all of these problems can be solved. We verified this with experiments showing that our method not only scales with heterogeneous data but even generalises across datasets, subjects, and tasks. Our method unlocks the potential of the bitter lesson, providing a general method to exploit more computation by using more data. We implore the research community to employ the vast quantities of data and compute available to realise this potential. If scale is all you need in speech decoding, then the bitter lesson may not be so bitter.

Acknowledgments and Disclosure of Funding

We would like to thank Botos Csaba for many insightful discussions and creative ideas which helped shaped the direction of this work. Thanks also to Minqi Jiang for an encouraging conversation on unsupervised representation learning, Mats W.J. van Es for technical assistance with the OSL library, Brian Liu for technical contributions which did not reach the final paper, and Miran Özdogan for reviewing a draft of this work. The authors would like to acknowledge the use of the University of Oxford Advanced Research Computing (ARC) facility in carrying out this work. <http://dx.doi.org/10.5281/zenodo.22558>.

DJ is supported by an AWS Studentship from the EPSRC CDT in Autonomous Intelligent Machines and Systems (AIMS). GL is supported by an EPSRC Studentship. MW is supported by the Wellcome Trust (106183/Z/14/Z, 215573/Z/19/Z), the New Therapeutics in Alzheimer’s Diseases (NTAD) study supported by UK MRC, the Dementia Platform UK (RG94383/RG89702) and the NIHR Oxford Health Biomedical Research Centre (NIHR203316). The views expressed are those of the author(s) and not necessarily those of the NIHR or the Department of Health and Social Care. OPJ is supported by the MRC (MR/X00757X/1), Royal Society (RG/R1/241267), NSF (2314493), NFRF (NFRFT-2022-00241), and SSHRC (895-2023-1022).

References

- [1] Pulkit Agrawal, João Carreira, and Jitendra Malik. Learning to see by moving. In *2015 IEEE International Conference on Computer Vision, ICCV 2015, Santiago, Chile, December 7-13, 2015*, pages 37–45. IEEE Computer Society, 2015. doi: 10.1109/ICCV.2015.13. URL <https://doi.org/10.1109/ICCV.2015.13>.
- [2] Kristijan Armeni, Umut Güçlü, Marcel van Gerven, and Jan-Mathijs Schoffelen. A 10-hour within-participant magnetoencephalography narrative dataset to test models of language comprehension. *Scientific Data*, 9(1):278, June 2022. ISSN 2052-4463. doi: 10.1038/s41597-022-01382-7. URL <https://www.nature.com/articles/s41597-022-01382-7>.
- [3] Randall Balestrieri, Mark Ibrahim, Vlad Sobal, Ari Morcos, Shashank Shekhar, Tom Goldstein, Florian Bordes, Adrien Bardes, Grégoire Mialon, Yuandong Tian, Avi Schwarzschild, Andrew Gordon Wilson, Jonas Geiping, Quentin Garrido, Pierre Fernandez, Amir Bar, Hamed Pirsiavash, Yann LeCun, and Micah Goldblum. A cookbook of self-supervised learning. *CoRR*, abs/2304.12210, 2023. doi: 10.48550/ARXIV.2304.12210. URL <https://doi.org/10.48550/arXiv.2304.12210>.
- [4] Florian Bordes, Samuel Lavoie, Randall Balestrieri, Nicolas Ballas, and Pascal Vincent. A surprisingly simple technique to control the pretraining bias for better transfer: Expand or narrow your representation. *CoRR*, abs/2304.05369, 2023. doi: 10.48550/ARXIV.2304.05369. URL <https://doi.org/10.48550/arXiv.2304.05369>.
- [5] Steven L Bressler and Craig G Richter. Interareal oscillatory synchronization in top-down neocortical processing. *Current Opinion in Neurobiology*, 31:62–66, 2015.
- [6] György Buzsáki and Xiao-Jing Wang. Mechanisms of gamma oscillations. *Annual Review of Neuroscience*, 35:203–225, 2012.
- [7] Mathilde Caron, Hugo Touvron, Ishan Misra, Hervé Jégou, Julien Mairal, Piotr Bojanowski, and Armand Joulin. Emerging properties in self-supervised vision transformers. In *2021 IEEE/CVF International Conference on Computer Vision, ICCV 2021, Montreal, QC, Canada, October 10-17, 2021*, pages 9630–9640. IEEE, 2021. doi: 10.1109/ICCV48922.2021.00951. URL <https://doi.org/10.1109/ICCV48922.2021.00951>.
- [8] Ting Chen, Simon Kornblith, Mohammad Norouzi, and Geoffrey E. Hinton. A simple framework for contrastive learning of visual representations. In *Proceedings of the 37th International Conference on Machine Learning, ICML 2020, 13-18 July 2020, Virtual Event*, volume 119 of *Proceedings of Machine Learning Research*, pages 1597–1607. PMLR, 2020. URL <http://proceedings.mlr.press/v119/chen20j.html>.
- [9] Xupeng Chen, Ran Wang, Amirhossein Khalilian-Gourtani, Leyao Yu, Patricia Dugan, Daniel Friedman, Werner Doyle, Orrin Devinsky, Yao Wang, and Adeen Flinker. A neural speech decoding framework leveraging deep learning and speech synthesis. *Nature Machine Intelligence*, pages 1–14, April 2024. ISSN 2522-5839. doi: 10.1038/s42256-024-00824-8. URL <https://www.nature.com/articles/s42256-024-00824-8>.

[10] Connie Cheung, Liberty S Hamilton, Keith Johnson, and Edward F Chang. The auditory representation of speech sounds in human motor cortex. *eLife*, 5:e12577, 2016.

[11] Richard Csaky, Mats W. J. van Es, Oiwi Parker Jones, and Mark W. Woolrich. Group-level brain decoding with deep learning. *Human Brain Mapping*, 44:6105 – 6119, 2022. URL <https://doi.org/10.1002/hbm.26500>.

[12] Richard Csaky, Mats W.J. van Es, Oiwi Parker Jones, and Mark Woolrich. Interpretable many-class decoding for MEG. *NeuroImage*, 282:120396, November 2023. ISSN 10538119. doi: 10.1016/j.neuroimage.2023.120396. URL <https://linkinghub.elsevier.com/retrieve/pii/S1053811923005475>.

[13] Debadatta Dash, Paul Ferrari, Satwik Dutta, and Jun Wang. NeuroVAD: Real-Time Voice Activity Detection from Non-Invasive Neuromagnetic Signals. *Sensors*, 20(8):2248, January 2020. ISSN 1424-8220. doi: 10.3390/s20082248. URL <https://www.mdpi.com/1424-8220/20/8/2248>.

[14] Alexandre Défossez, Jade Copet, Gabriel Synnaeve, and Yossi Adi. High fidelity neural audio compression. *CoRR*, abs/2210.13438, 2022. doi: 10.48550/ARXIV.2210.13438. URL <https://doi.org/10.48550/arXiv.2210.13438>.

[15] Carl Doersch, Abhinav Gupta, and Alexei A. Efros. Unsupervised visual representation learning by context prediction. In *2015 IEEE International Conference on Computer Vision, ICCV 2015, Santiago, Chile, December 7-13, 2015*, pages 1422–1430. IEEE Computer Society, 2015. doi: 10.1109/ICCV.2015.167. URL <https://doi.org/10.1109/ICCV.2015.167>.

[16] Yiqun Duan, Charles Chau, Zhen Wang, Yu-Kai Wang, and Chin-Teng Lin. DeWave: Discrete encoding of EEG waves for EEG to text translation. In Alice Oh, Tristan Naumann, Amir Globerson, Kate Saenko, Moritz Hardt, and Sergey Levine, editors, *Advances in Neural Information Processing Systems 36 (NeurIPS 2023), New Orleans, LA, USA, December 10 - 16, 2023*. URL http://papers.nips.cc/paper_files/paper/2023/hash/1f2fd23309a5b2d2537d063b29ec1b52-Abstract-Conference.html.

[17] Alexandre Défossez, Charlotte Caucheteux, Jérémie Rapin, Ori Kabeli, and Jean-Rémi King. Decoding speech perception from non-invasive brain recordings. *Nature Machine Intelligence*, 5(10):1097–1107, October 2023. ISSN 2522-5839. doi: 10.1038/s42256-023-00714-5. URL <https://www.nature.com/articles/s42256-023-00714-5>.

[18] Pascal Fries. A mechanism for cognitive dynamics: neuronal communication through neuronal coherence. *Trends in Cognitive Sciences*, 9(10):474–480, October 2005. ISSN 1364-6613. doi: 10.1016/j.tics.2005.08.011. URL <https://www.sciencedirect.com/science/article/pii/S1364661305002421>.

[19] Pascal Fries. Neuronal gamma-band synchronization as a fundamental process in cortical computation. *Annual Review of Neuroscience*, 32:209–224, 2009.

[20] Andrew Gibiansky, Sercan Ömer Arik, Gregory Frederick Diamos, John Miller, Kainan Peng, Wei Ping, Jonathan Raiman, and Yanqi Zhou. Deep voice 2: Multi-speaker neural text-to-speech. In Isabelle Guyon, Ulrike von Luxburg, Samy Bengio, Hanna M. Wallach, Rob Fergus, S. V. N. Vishwanathan, and Roman Garnett, editors, *Advances in Neural Information Processing Systems 30: Annual Conference on Neural Information Processing Systems 2017, December 4-9, 2017, Long Beach, CA, USA*, pages 2962–2970, 2017. URL <https://proceedings.neurips.cc/paper/2017/hash/c59b469d724f7919b7d35514184fdc0f-Abstract.html>.

[21] Spyros Gidaris, Praveer Singh, and Nikos Komodakis. Unsupervised representation learning by predicting image rotations. In *6th International Conference on Learning Representations, ICLR 2018, Vancouver, BC, Canada, April 30 - May 3, 2018, Conference Track Proceedings*. OpenReview.net, 2018. URL <https://openreview.net/forum?id=S1v4N210->.

[22] Anne-Lise Giraud and David Poeppel. Cortical oscillations and speech processing: emerging computational principles and operations. *Nature Neuroscience*, 15(4):511–517, April 2012. ISSN 1546-1726. doi: 10.1038/nn.3063. URL <https://www.nature.com/articles/nn.3063>.

[23] Laura Gwilliams, Jean-Rémi King, Alec Marantz, and David Poeppel. Neural dynamics of phoneme sequences reveal position-invariant code for content and order. *Nature Communications*, 13(1):6606, November 2022. ISSN 2041-1723. doi: 10.1038/s41467-022-34326-1. URL <https://www.nature.com/articles/s41467-022-34326-1>.

[24] Laura Gwilliams, Graham Flick, Alec Marantz, Liina Pylkkänen, David Poeppel, and Jean-Rémi King. Introducing MEG-MASC a high-quality magneto-encephalography dataset for evaluating natural speech processing. *Scientific Data*, 10(1):862, December 2023. ISSN 2052-4463. doi: 10.1038/s41597-023-02752-5. URL <https://www.nature.com/articles/s41597-023-02752-5>.

[25] Emma L. Hall, Siân E. Robson, Peter G. Morris, and Matthew J. Brookes. The relationship between MEG and fMRI. *NeuroImage*, 102:80–91, 2014. URL <https://doi.org/10.1016/j.neuroimage.2013.11.005>.

[26] Liberty S. Hamilton, Erik Edwards, and Edward F. Chang. A Spatial Map of Onset and Sustained Responses to Speech in the Human Superior Temporal Gyrus. *Current Biology*, 28(12):1860–1871.e4, June 2018. ISSN 09609822. doi: 10.1016/j.cub.2018.04.033. URL <https://linkinghub.elsevier.com/retrieve/pii/S0960982218304615>.

[27] Weibang Jiang, Liming Zhao, and Bao liang Lu. Large brain model for learning generic representations with tremendous EEG data in BCI. In *The Twelfth International Conference on Learning Representations*, 2024. URL <https://openreview.net/forum?id=QzTpTRVtrP>.

[28] Hyejeong Jo, Yiqian Yang, Juhyeok Han, Yiqun Duan, Hui Xiong, and Won Hee Lee. Are EEG-to-text models working? *arXiv*, 2024. doi: <https://arxiv.org/abs/2405.06459>.

[29] John M. Jumper, Richard Evans, Alexander Pritzel, Tim Green, Michael Figurnov, Olaf Ronneberger, Kathryn Tunyasuvunakool, Russ Bates, Augustin Žídek, Anna Potapenko, Alex Bridgland, Clemens Meyer, Simon A A Kohl, Andy Ballard, Andrew Cowie, Bernardino Romera-Paredes, Stanislav Nikolov, Rishabh Jain, Jonas Adler, Trevor Back, Stig Petersen, David Reiman, Ellen Clancy, Michal Zielinski, Martin Steinegger, Michalina Pacholska, Tamas Berghammer, Sebastian Bodenstein, David Silver, Oriol Vinyals, Andrew W. Senior, Koray Kavukcuoglu, Pushmeet Kohli, and Demis Hassabis. Highly accurate protein structure prediction with alphafold. *Nature*, 596:583 – 589, 2021. URL <https://doi.org/10.1038/s41586-021-03819-2>.

[30] Peter Langland-Hassan and Agustín Vicente. *Inner Speech: New Voices*. Oxford University Press, 2018.

[31] Gustav Larsson, Michael Maire, and Gregory Shakhnarovich. Learning representations for automatic colorization. In Bastian Leibe, Jiri Matas, Nicu Sebe, and Max Welling, editors, *Computer Vision - ECCV 2016 - 14th European Conference, Amsterdam, The Netherlands, October 11-14, 2016, Proceedings, Part IV*, volume 9908 of *Lecture Notes in Computer Science*, pages 577–593. Springer, 2016. doi: 10.1007/978-3-319-46493-0_35. URL https://doi.org/10.1007/978-3-319-46493-0_35.

[32] Fernando Lopes da Silva. EEG and MEG: Relevance to Neuroscience. *Neuron*, 80(5):1112–1128, December 2013. ISSN 0896-6273. doi: 10.1016/j.neuron.2013.10.017. URL <https://www.sciencedirect.com/science/article/pii/S0896627313009203>.

[33] Ilya Loshchilov and Frank Hutter. Decoupled weight decay regularization. In *7th International Conference on Learning Representations, ICLR 2019, New Orleans, LA, USA, May 6-9, 2019*. OpenReview.net, 2019. URL <https://openreview.net/forum?id=Bkg6RiCqY7>.

[34] Huan Luo and David Poeppel. Phase patterns of neuronal responses reliably discriminate speech in human auditory cortex. *Neuron*, 54(6):1001–1010, 2007.

[35] Huan Luo, Zuxiang Liu, and David Poeppel. Auditory cortex tracks both auditory and visual stimulus dynamics using low-frequency neuronal phase modulation. *PLOS Biology*, 8(8):e1000445, 2010.

[36] Guangting Mai, James W. Minett, and William S. Y. Wang. Delta, theta, beta, and gamma brain oscillations index levels of auditory sentence processing. *NeuroImage*, 133:516–528, June 2016. ISSN 1053-8119. doi: 10.1016/j.neuroimage.2016.02.064. URL <https://www.sciencedirect.com/science/article/pii/S1053811916001737>.

[37] Stéphanie Martin, Peter Brunner, Chris Holdgraf, Hans-Jochen Heinze, Nathan E Crone, Jochem Rieger, Gerwin Schalk, Robert T Knight, and Brian N Pasley. Decoding spectrotemporal features of overt and covert speech from the human cortex. *Frontiers in Neuroengineering*, 7:14, 2014.

[38] Nima Mesgarani, Connie Cheung, Keith Johnson, and Edward F. Chang. Phonetic feature encoding in human superior temporal gyrus. *Science*, 343(6174):1006–1010, 2014. doi: DOI:10.1126/science.1245994.

[39] Sean L. Metzger, Kaylo T. Littlejohn, Alexander B. Silva, David A. Moses, Margaret P. Seaton, Ran Wang, Maximilian E. Dougherty, Jessie R. Liu, Peter Wu, Michael A. Berger, Inga Zhuravleva, Adelyn Tu-Chan, Karunesh Ganguly, Gopala K. Anumanchipalli, and Edward F. Chang. A high-performance neuroprosthesis for speech decoding and avatar control. *Nature*, 620:1037–1046, 2023.

[40] David A. Moses, Sean L. Metzger, Jessie R. Liu, Gopala K. Anumanchipalli, Joseph G. Makin, Pengfei F. Sun, Josh Chartier, Maximilian E. Dougherty, Patricia M. Liu, Gary M. Abrams, Adelyn Tu-Chan, Karunesh Ganguly, and Edward F. Chang. Neuroprosthesis for Decoding Speech in a Paralyzed Person with Anarthria. *New England Journal of Medicine*, 385(3):217–227, July 2021. ISSN 0028-4793. doi: 10.1056/NEJMoa2027540. URL <https://doi.org/10.1056/NEJMoa2027540>.

[41] Mehdi Noroozi and Paolo Favaro. Unsupervised learning of visual representations by solving jigsaw puzzles. In Bastian Leibe, Jiri Matas, Nicu Sebe, and Max Welling, editors, *Computer Vision - ECCV 2016 - 14th European Conference, Amsterdam, The Netherlands, October 11-14, 2016, Proceedings, Part VI*, volume 9910 of *Lecture Notes in Computer Science*, pages 69–84. Springer, 2016. doi: 10.1007/978-3-319-46466-4_5. URL https://doi.org/10.1007/978-3-319-46466-4_5.

[42] OpenAI. GPT-4 technical report. *CoRR*, abs/2303.08774, 2023. doi: 10.48550/ARXIV.2303.08774. URL <https://doi.org/10.48550/arXiv.2303.08774>.

[43] Jonathan E. Peelle, Joachim Gross, and Matthew H. Davis. Phase-locked responses to speech in human auditory cortex are enhanced during comprehension. *Cerebral Cortex*, 23(6):1378–1387, 2012.

[44] Ethan Perez, Florian Strub, Harm de Vries, Vincent Dumoulin, and Aaron C. Courville. FiLM: Visual reasoning with a general conditioning layer. In Sheila A. McIlraith and Kilian Q. Weinberger, editors, *Proceedings of the Thirty-Second AAAI Conference on Artificial Intelligence, (AAAI-18), the 30th innovative Applications of Artificial Intelligence (IAAI-18), and the 8th AAAI Symposium on Educational Advances in Artificial Intelligence (EAAI-18), New Orleans, Louisiana, USA, February 2-7, 2018*, pages 3942–3951. AAAI Press, 2018. doi: 10.1609/AAAI.V32I1.11671. URL <https://doi.org/10.1609/aaai.v32i1.11671>.

[45] Vitória Piai, Ardi Roelofs, and Eric Maris. Oscillatory brain responses in spoken word production reflect lexical frequency and sentential constraint. *Neuropsychologia*, 53:146–156, January 2014. ISSN 0028-3932. doi: 10.1016/j.neuropsychologia.2013.11.014. URL <https://www.sciencedirect.com/science/article/pii/S0028393213004119>.

[46] Alec Radford, Jong Wook Kim, Tao Xu, Greg Brockman, Christine McLeavey, and Ilya Sutskever. Robust speech recognition via large-scale weak supervision. In *International Conference on Machine Learning, ICML 2023, 23-29 July 2023, Honolulu, Hawaii, USA*, volume 202 of *Proceedings of Machine Learning Research*, pages 28492–28518. PMLR, 2023. URL <https://proceedings.mlr.press/v202/radford23a.html>.

[47] Jan-Mathijs Schoffelen, Robert Oostenveld, Nietzsche H. L. Lam, Julia Uddén, Annika Hultén, and Peter Hagoort. A 204-subject multimodal neuroimaging dataset to study language processing. *Scientific Data*, 6(1):17, April 2019. ISSN 2052-4463. doi: 10.1038/s41597-019-0020-y. URL <https://www.nature.com/articles/s41597-019-0020-y>.

[48] Meredith A. Shafto, Lorraine K. Tyler, Marie Dixon, Jason R. Taylor, James Benedict Rowe, Rhodri Cusack, Andrew J. Calder, William D. Marslen-Wilson, John S. Duncan, T. Dalgleish, Richard N. A. Henson, Carol Brayne, and Fiona E. Matthews. The Cambridge centre for ageing and neuroscience (Cam-CAN) study protocol: a cross-sectional, lifespan, multidisciplinary examination of healthy cognitive ageing. *BMC Neurology*, 14, 2014.

[49] Antje Strauß, Molly J Henry, Mathias Scharinger, and Jonas Obleser. Alpha phase determines successful lexical decision in noise. *Journal of Neuroscience*, 35(7):3256–3262, 2015.

[50] Richard Sutton. The bitter lesson. *Incomplete Ideas (blog)*, 2019. URL <http://www.incompleteideas.net/IncIdeas/BitterLesson.html>.

[51] Marco Tagliasacchi, Yunpeng Li, Karolis Misiunas, and Dominik Roblek. SEANet: A multi-modal speech enhancement network. In Helen Meng, Bo Xu, and Thomas Fang Zheng, editors, *Interspeech 2020, 21st Annual Conference of the International Speech Communication Association, Virtual Event, Shanghai, China, 25-29 October 2020*, pages 1126–1130. ISCA, 2020. doi: 10.21437/INTERSPEECH.2020-1563. URL <https://doi.org/10.21437/Interspeech.2020-1563>.

[52] Jerry Tang, Amanda LeBel, Shailee Jain, and Alexander G. Huth. Semantic reconstruction of continuous language from non-invasive brain recordings. *Nature Neuroscience*, 26(5):858–866, May 2023. ISSN 1546-1726. doi: 10.1038/s41593-023-01304-9. URL <https://www.nature.com/articles/s41593-023-01304-9>.

[53] Jason R. Taylor, Nitin Williams, Rhodri Cusack, Tibor Auer, Meredith A. Shafto, Marie Dixon, Lorraine K. Tyler, Cam-CAN Group, and Richard N. A. Henson. The Cambridge centre for ageing and neuroscience (Cam-CAN) data repository: Structural and functional MRI, MEG, and cognitive data from a cross-sectional adult lifespan sample. *Neuroimage*, 144:262 – 269, 2017.

[54] Diego Vidaurre, Laurence T. Hunt, Andrew J. Quinn, Benjamin A. E. Hunt, Matthew J. Brookes, Anna C. Nobre, and Mark W. Woolrich. Spontaneous cortical activity transiently organises into frequency specific phase-coupling networks. *Nature Communications*, 9(1):2987, July 2018. ISSN 2041-1723. doi: 10.1038/s41467-018-05316-z. URL <https://www.nature.com/articles/s41467-018-05316-z>.

[55] Sarah K Wandelt, David A. Bjånes, Kelsie Pejsa, Brian Lee, Charles Y Liu, and Richard Andersen. Representation of internal speech by single neurons in human supramarginal gyrus. *Nature human behaviour*, 2024. URL <https://doi.org/10.1038/s41562-024-01867-y>.

[56] Bo Wang, Xiran Xu, Longxiang Zhang, Boda Xiao, Xihong Wu, and Jing Chen. Semantic reconstruction of continuous language from MEG signals. *CoRR*, abs/2309.07701, 2023. doi: 10.48550/ARXIV.2309.07701. URL <https://doi.org/10.48550/arXiv.2309.07701>.

[57] Christopher Wang, Vighnesh Subramaniam, Adam Uri Yaari, Gabriel Kreiman, Boris Katz, Ignacio Cases, and Andrei Barbu. Brainbert: Self-supervised representation learning for intracranial recordings. In *The Eleventh International Conference on Learning Representations, ICLR 2023, Kigali, Rwanda, May 1-5, 2023*. OpenReview.net, 2023. URL https://openreview.net/pdf?id=xmcYx_reUn6.

[58] Zhenhailong Wang and Heng Ji. Open vocabulary electroencephalography-to-text decoding and zero-shot sentiment classification. In *Thirty-Sixth AAAI Conference on Artificial Intelligence, AAAI 2022, Virtual Event, February 22 - March 1*, pages 5350–5358. AAAI Press, 2022. doi: 10.1609/AAAI.V36I5.20472. URL <https://doi.org/10.1609/aaai.v36i5.20472>.

[59] Sabine Weiss and Horst M. Mueller. “Too many betas do not spoil the broth”: the role of beta brain oscillations in language processing. *Frontiers in Psychology*, 3, 2012. doi: <https://doi.org/10.3389/fpsyg.2012.00201>.

[60] Francis R. Willett, Erin M. Kunz, Chaofei Fan, Donald T. Avansino, Guy H. Wilson, Eun Young Choi, Foram Kamdar, Matthew F. Glasser, Leigh R. Hochberg, Shaul Druckmann, Krishna V. Shenoy, and Jaimie M. Henderson. A high-performance speech neuroprosthesis. *Nature*, 620(7976):1031–1036, August 2023. ISSN 1476-4687. doi: 10.1038/s41586-023-06377-x. URL <https://www.nature.com/articles/s41586-023-06377-x>.

[61] Neil Zeghidour, Alejandro Luebs, Ahmed Omran, Jan Skoglund, and Marco Tagliasacchi. Soundstream: An end-to-end neural audio codec. *IEEE ACM Trans. Audio Speech Lang. Process.*, 30:495–507, 2022. doi: 10.1109/TASLP.2021.3129994. URL <https://doi.org/10.1109/TASLP.2021.3129994>.

[62] Richard Zhang, Phillip Isola, and Alexei A. Efros. Colorful image colorization. In Bastian Leibe, Jiri Matas, Nicu Sebe, and Max Welling, editors, *Computer Vision - ECCV 2016 - 14th European Conference, Amsterdam, The Netherlands, October 11-14, 2016, Proceedings, Part III*, volume 9907 of *Lecture Notes in Computer Science*, pages 649–666. Springer, 2016. doi: 10.1007/978-3-319-46487-9_40. URL https://doi.org/10.1007/978-3-319-46487-9_40.

A Supervised Heard Speech Decoding

While this work is primarily about *scaling* speech decoding, we also set the first baselines for speech detection and voicing classification from MEG with connected auditory speech stimuli. Therefore, in this section we provide fully supervised results where our architecture is trained to completion using all available labelled data in the corresponding dataset (except the validation and test splits) and compare this to a linear classifier baseline. These results are not comparable with our self-supervised models because the entire architecture is trained end-to-end. In our SSL work with shallow fine-tuning, only the final classifier is trained with labels.

Table 3: **Supervised baselines.** Uncertainty is standard error of the mean over three random seeds.

Experiment	Balanced accuracy	
	Speech detection	Voicing
Armeni (linear)	0.5222 ± 0.0015	0.5207 ± 0.0007
Armeni (ours)	0.7253 ± 0.0005	0.5282 ± 0.0006
Gwilliams (linear)	0.5006 ± 0.0001	0.5166 ± 0.0002
Gwilliams (ours)	0.5946 ± 0.0016	0.5211 ± 0.0005

The results in Table 3 show that we can achieve strong speech detection results on Armeni et al. [2] and Gwilliams et al. [24] with our architecture. The difference between the two may be due to a combination of different scanners, numbers of sensors (208 vs 269 magnetometers), varied difficulty in the audio stimulus, and more within-subject data in Armeni et al. [2]. We also achieve good results on voicing classification for both datasets, easily outperforming the linear models.

One potential way to improve on both supervised and self-supervised approaches is by using a temporally aware model such as an LSTM or an attentional model such as a Transformer as the classifier. We do not investigate this within this paper as it is out of scope. Rather, we choose to use simple classifiers as the purpose of this paper is to demonstrate the potential of scaling.

B Subject Conditioning

To investigate subject conditioning approaches, we pre-train then fine-tune our models on a subset of Gwilliams et al. [24], holding out three subjects for evaluation. We conduct these experiments without conditioning, with subject embeddings, and with FiLM to see if they have any influence on subject generalisation. We represent embeddings as learnable vectors, unique to each subject, that are concatenated to the backbone representation. For FiLM, we use the same embeddings as inputs to the functions that modulate the backbone representation.

Table 4: **Subject conditioning improves generalisation on seen subjects but not novel subjects.** We quote test accuracy at the point of best validation accuracy (early stopping). Uncertainty is the standard error of the mean and we show the *t*-score and *p*-value from a one-sample one-sided *t*-test where the population mean is chance-level accuracy.

Subject conditioning	Seen	Subject voicing balanced accuracy				
		<i>t</i>	<i>p</i>	Unseen (zero-shot)	<i>t</i>	<i>p</i>
None	0.5118 ± 0.001	8.4	0.007	0.5057 ± 0.001	4.5	0.02
Embedding	0.5168 ± 0.0006	27.9	0.0006	0.5052 ± 0.0007	7.5	0.009
FiLM [44]	0.5197 ± 0.001	18.6	0.001	0.5058 ± 0.002	3.3	0.04
Chance-level	0.5	—	—	0.5	—	—

Table 4 reveals that in-distribution subject generalisation is helped by using subject conditioning methods. Both subject embeddings and FiLM conditioning outperform no conditioning, with FiLM being best. However, for novel subject generalisation, using a subject conditioning method makes little difference. Regardless of conditioning, we can generalise beyond chance-level, but suffer a reduction in accuracy compared to in-distribution subjects. Conditioning may be negligible in the unseen case as the embeddings are random rather than learned for the held-out subjects.

C Aggregating Unlabelled Datasets

To scale up unlabelled data further than individual studies, we must be able to combine many existing datasets. As a preliminary investigation, we combine two of the largest public MEG datasets: MOUS [47] and Cam-CAN [48, 53]. We investigate how pre-training with these combined datasets affects downstream performance using the same experimental setup as Figure 3.

Table 5: **Combining two unlabelled datasets does not improve over the best study.** We quote test accuracy at the point of best validation accuracy (early stopping). The uncertainty is the standard error of the mean calculated over three seeds.

Labels	Pre-training data (hours)	Balanced accuracy	
		Speech detection	Voicing
Armeni	MOUS (160 hours)	0.5736 ± 0.0016	0.5220 ± 0.0013
	Cam-CAN (159 hours)	0.5911 ± 0.0009	0.5241 ± 0.0004
	Cam-CAN + MOUS (319 hours)	0.5872 ± 0.0012	0.5236 ± 0.0016
Gwilliams	MOUS (160 hours)	0.5060 ± 0.0006	0.5175 ± 0.0008
	Cam-CAN (159 hours)	0.5118 ± 0.0011	0.5196 ± 0.0010
	Cam-CAN + MOUS (319 hours)	0.5116 ± 0.0017	0.5187 ± 0.0013

The results in Table 5 suggest that combining these two datasets is not strictly better than the best dataset on its own. Pre-training on Cam-CAN alone leads to the best performance in all instances. This suggests that Cam-CAN is a better pre-training dataset than MOUS—a surprising result given that MOUS and Armeni et al. [2] share the same scanning hardware and MOUS includes data from subjects listening to speech while Cam-CAN has no such language tasks. This could be due to Cam-CAN being a cleaner dataset as we found artefacts can significantly affect learning. Combining Cam-CAN with MOUS performs marginally worse or the same as Cam-CAN alone. For all but one instance they are within the standard error of the mean of each other. The combined datasets always outperform MOUS on its own.

In general, further investigation is necessary to determine how datasets should be best aggregated. Increasing the number of datasets could enable the network to model the variance between them and eventually improve over the best singular dataset. This remains an open question as we were only able to study up to two datasets in this paper.

D Task Labels Are Hard To Scale; Generic SSL Scales Best

Our self-supervised tasks led to clearly generalisable and scalable representations by providing an inductive bias towards speech decoding. However, could these representations be made more powerful by utilising labels from other speech decoding tasks to improve this bias? This moves us into the *semi-supervised learning* regime, where we use a mix of labelled and unlabelled data.

With the same experimental setup as Figure 3, we add speech detection or voicing as an additional loss during pre-training. Figure 5 shows that no amount of additional labelled data improves downstream accuracy, with all data points remaining near the range of the standard error of the mean of the SSL baseline for both tasks. There also does not appear to be any indication of scaling within the range of labelled data available to us.

This outcome indicates that our self-supervised losses are the main contributor to downstream accuracy. The MEG signal appears rich, encapsulating lots of information, with the speech component being a subset distributed across the representation space. Learning with specific labels produces representations that are too specialised to improve on other speech decoding tasks. This does not preclude there being some—or a combination of—labelled tasks that provide more general inductive biases for speech; nor does it mean more labelled data will not scale. However, the point remains salient. Labelled data is more difficult to scale given its scarcity and the generic property is lost with specific labels while it is well-preserved with SSL, providing another reminder of the bitter lesson.

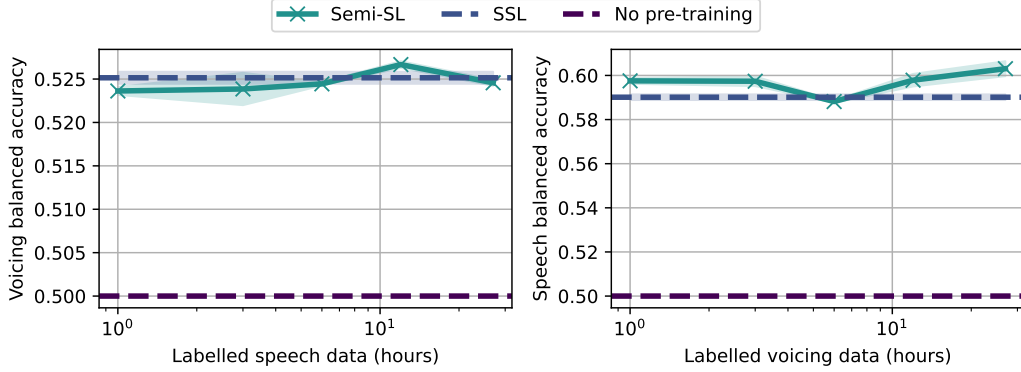


Figure 5: **Cross-task semi-supervised learning does not improve generalisation.** We pre-train with increasing amounts of labelled data from Armeni et al. [2], using speech labels when evaluating voicing and voicing labels for speech. We also use a constant 38 hours of unlabelled data in pre-training. *No pre-training* shows test accuracy for a randomly initialised network fine-tuned for the same number of epochs (i.e. without pre-training). *SSL* is when pre-training with *only* the unlabelled data. The shaded area shows the standard error of the mean across three seeds.

E Experiment Details

To generate the data in Table 1, we pre-train our representations with non-overlapping sample windows from all subjects and sessions 001 to 009 of Armeni et al. [2] for 200 epochs with a 0.8 : 0.1 : 0.1 train/val/test split. We shallow fine-tune with labels for 30 epochs using all subjects, but only session 010, which was held-out during pre-training.

For the data in Figure 3, we use the same number of epochs and the same ratios for data splitting. We pre-train only with Cam-CAN [48, 53]. We adjust the amount of unlabelled data used by increasing the number of subjects in the sequence 1, 2, 4, 8, 17, 36, 74, 152, 312, and 641, successively randomly selecting more subjects to include. Each seed uses a different set of subjects to reduce negative effects from outlier subjects. We fine-tune with all data in Armeni et al. [2] and Gwilliams et al. [24] with the same train/val/test ratios as before.

For the results shown in Figure 5, we use the same setup as in Figure 3. In addition to the unlabelled data, we add labelled data from Armeni et al. [2], increasing the number of sessions used in the sequence 1, 3, 6, 9, 12, and 27. For this experiment, we calculate the number of labelled data hours using an estimate of 1 hour per session per subject.

Finally, for the results in Table 4, we pre-train and deep fine-tune to saturation with subjects 01-07 of Gwilliams et al. [24] and test zero-shot generalisation using held-out subjects 08-10. All other experimental details are the same as the previous two experiments.

In all experiments, we use three randomly selected seeds for each pre-training and corresponding fine-tuning run. For speech detection, since our encoder reduces the temporal dimension from 125 samples (the number of samples in a 0.5 second window with a sample rate of 250Hz) down to 5 embeddings, we downsample our speech detection labels to match using PyTorch’s `torch.nn.functional.interpolate`. Therefore, each speech detection label represents a 0.1 second period of time.

F Hyperparameters

We conduct a search over hyperparameters of interest to optimise our self-supervised objectives and neural architecture. In all experiments in this section, we measure downstream performance (using shallow fine-tuning) with best validation accuracy for speech detection unless explicitly specified, training and evaluating only on data from subject 001 of Armeni et al. [2] to minimise training time, over three random seeds. All uncertainties in this section are standard deviations and not standard error of the mean as in the main body.

Table 6 shows the results of a search over the proportion ρ of sensors to apply the phase and amplitude pretext task transformations to. We only search up to $\rho = 0.5$ as anything above this is equivalent to applying the inverse transformation to a proportion $1 - \rho$ of the sensors. We find that for phase shift prediction, $\rho = 0.5$ is optimal, while for amplitude scale prediction $\rho = 0.2$ is best.

Table 6: **Best ρ for phase and amplitude pretext tasks.**

Task	ρ	Balanced accuracy
Phase shift prediction	0.1	0.5452 ± 0.0048
	0.2	0.5566 ± 0.0014
	0.3	0.5578 ± 0.0021
	0.4	0.5530 ± 0.0014
	0.5	0.5655 ± 0.0026
Amplitude scale prediction	0.1	0.5440 ± 0.0012
	0.2	0.5796 ± 0.0050
	0.3	0.5625 ± 0.0063
	0.4	0.5684 ± 0.0016
	0.5	0.5650 ± 0.0026

In our architecture, we define d_{backbone} to be the bottleneck dimension of the cortex encoder (i.e. the embedding dimension) as well as the size of d_{shared} . Balestrieri et al. [3], using the results from work by Bordes et al. [4], suggest that increasing the backbone output dimension in self-supervised learning leads to better downstream transfer. We investigate this for our architecture by varying the encoder dimension in Table 7. Our results are consistent with their findings. Balanced accuracy is highest at the largest encoder dimension we evaluated. Encoder dimensions larger than 2048 led to unstable training and were not feasible given the compute resources available to us.

Table 7: **Optimal encoder dimension.**

d_{backbone}	Balanced accuracy
128	0.5775 ± 0.0037
300	0.5715 ± 0.0012
512	0.5835 ± 0.0016
1024	0.5800 ± 0.0050
2048	0.5987 ± 0.0024

In Table 8, we show the effect of varying the length w , i.e. the window size of each data sample. Increasing the window to five seconds led to unstable losses in pre-training so we did not evaluate above a window length of two seconds. This is likely to be because increasing the window size reduces the number of training samples when only non-overlapping samples are used. For speech detection, there appears to be a U-shaped distribution, where very short and very long windows lead to better downstream accuracy. For voicing classification, the window lengths we evaluated seem to make little difference. However, windows smaller than 0.1 seconds may lead to significantly lower accuracy as most phonemes will occur for at least this length of time in the neural response [23].

Table 8: **Ideal sample window length.**

Window length (s)	Balanced accuracy	
	Speech detection	Voicing classification
0.2	0.5919 ± 0.0014	0.5033 ± 0.0014
0.4	0.5804 ± 0.0036	0.5077 ± 0.0027
0.5	0.5715 ± 0.0012	0.5055 ± 0.0023
1.0	0.5790 ± 0.0012	0.5062 ± 0.0020
2.0	0.6116 ± 0.0019	0.5065 ± 0.0011

We also evaluated several different configurations of the SEANet architecture for the cortex encoder, converging on convolutional blocks with channel dimensions (512, 512, 512, 512).

While these ablations indicate a theoretically ideal architectural configuration, in practice, we altered our final experimental architecture due to instabilities during training when data was scaled up. Our final architecture hyperparameters achieve a balance between the best values from our hyperparameter search and stable training. These values are detailed in Table 9.

Table 9: **Experimental hyperparameters.**

Hyperparameter	Value
Window length (s)	0.5
ρ (phase)	0.5
ρ (amplitude)	0.2
$\{w_1, w_2, w_3\}$	$\{1.0, 1.0, 1.0\}$
d_{shared}	512
d_{backbone}	512
SEANet convolution channels	(512, 512, 512, 512)
SEANet downsampling ratios	(5, 5, 1)
FiLM conditioning dimension	16
Subject embedding dimension	16
Pre-training epochs	200
Optimizer	AdamW [33]
Learning rate	0.000066
Train ratio	0.8
Validation ratio	0.1
Test ratio	0.1

G Compute Resources

All experiments were run on individual NVIDIA V100 and A100 GPUs with up to 40GiB of GPU memory on a system with up to 1TiB of RAM. Each pre-training run with the maximum amount of pre-training data took approximately 200 hours (8.3 days). Fine-tuning following pre-training took up to another 12 hours. We estimate that we used approximately 3000 hours of compute for the final experimental runs, including hyperparameter searches. In total, over the course of developing this work from idea to final paper, we used around 10,000 hours of GPU compute.

H Licences For Datasets And Code

The Armeni et al. [2] dataset is distributed under CC-BY-4.0 while the Gwilliams et al. [24] dataset is distributed under the CC0 1.0 Universal licence. The Schoffelen et al. [47] dataset is distributed with a RU-DI-HD-1.0 licence from the Donders institute. The licence for the Cam-CAN [48, 53] dataset is unknown. The SEANet code adapted from Défossez et al. [14] is distributed under the MIT licence, and the OSL library, which we use for preprocessing, is under the BSD-3-Clause licence.

I Broader Impacts

Decoding speech from non-invasive brain recordings is likely to bring about significant positive societal impacts. Research in this field could enable paralysed patients to communicate freely and materially assist those with minor communication difficulty (e.g. stammering). As the technology matures, it could also enable new ways of communicating with others and interacting with devices without the risks of invasive surgical implants. Nevertheless, the maturity of this technology could also present potential negative societal impacts. For one, reading inner speech creates new concerns over data controls as this information is likely to be highly sensitive and personal to individuals. Given access to this technology, there is also the risk that bad actors could extract sensitive information from target individuals without consent. Moreover, there are possible long horizon effects associated with speech decoding research. Broad adoption of this technology could lead to the gradual erosion of privacy over inner speech within society. In addition, asymmetric effects, where some individuals or organisations can read inner speech but others are unable to, could worsen societal inequality. Within the scope of this paper, we mitigate risks associated with inner speech by focusing on decoding heard speech where there is low potential for abuse. Nonetheless, we acknowledge that this is still a stepping stone towards solving inner speech decoding.